crystals

MDPI

Article

Growth and Spectroscopy of Yb:$YMgB_5O_{10}$ Crystal

Konstantin N. Gorbachenya [1], Anatol S. Yasukevich [1], Andrey I. Lazarchuk [1], Victor E. Kisel [1], Nikolay V. Kuleshov [1], Elena A. Volkova [2,*], Victor V. Maltsev [2], Elizaveta V. Koporulina [2,3], Vasiliy O. Yapaskurt [4], Nikolai N. Kuzmin [2,5,6], Dmitry A. Ksenofontov [2], Diana D. Mitina [2] and Anna I. Jiliaeva [2]

1 Center for Optical Materials and Technologies, Belarusian National Technical University, Nezalezhnasti Ave., 65, 220013 Minsk, Belarus; gorby@bntu.by (K.N.G.); anatol@bntu.by (A.S.Y.); lazartschuk1405@gmail.com (A.I.L.); vekisel@bntu.by (V.E.K.); nkuleshov@bntu.by (N.V.K.)
2 Department of Crystallography and Crystal Chemistry, Faculty of Geology, Moscow State University, 119234 Moscow, Russia; maltsev@geol.msu.ru (V.V.M.); e_koporulina@mail.ru (E.V.K.); kolyanfclm@mail.ru (N.N.K.); ksen53@gmail.com (D.A.K.); varya-mitya@mail.ru (D.D.M.); annajiliaeva@yandex.ru (A.I.J.)
3 Melnikov Research Institute of Comprehensive Exploitation of Mineral Resources of the Russian Academy of Sciences, 111020 Moscow, Russia
4 Laboratory of Local Methods for the Study of Matter, Faculty of Geology, Moscow State University, 119234 Moscow, Russia; vyapaskurt@mail.ru
5 Institute of Spectroscopy of Russian Academy of Science, Fizicheskaya Str. 5, 108840 Troitsk, Russia
6 Moscow Institute of Physics and Technology (National Research University), 9 Institutskiy Per., 141700 Dolgoprudny, Russia
* Correspondence: volkova@geol.msu.ru

Abstract: A transparent Yb:$YMgB_5O_{10}$ single crystal with dimensions up to 25 × 23 × 25 mm and weight 10.337 g was grown using a high-temperature solution growth on dipped seeds technique with a $K_2Mo_3O_{10}$ solvent. The Yb^{3+} concentration was calculated to be 4.7 at.% (N_{Yb} = 3.71 × 10^{20} atoms/cm^3) with a distribution coefficient K_d of 0.59. The grown crystal was characterized by means of PXRD, TGA-DSC and ATR-FTIR techniques. The spectroscopic characteristics of the Yb:$YMgB_5O_{10}$ crystal were demonstrated. Absorption cross-section spectra were produced. The luminescence spectra of the Yb:$YMgB_5O_{10}$ crystal were measured in the spectral range of 950–1100 nm. The luminescence kinetics of the $^2F_{5/2}$ energy level were investigated and the lifetime was determined.

Keywords: ytterbium; spectroscopy; rare-earth pentaborate; flux growth; ATR-FTIR spectroscopy

check for updates

Citation: Gorbachenya, K.N.; Yasukevich, A.S.; Lazarchuk, A.I.; Kisel, V.E.; Kuleshov, N.V.; Volkova, E.A.; Maltsev, V.V.; Koporulina, E.V.; Yapaskurt, V.O.; Kuzmin, N.N.; et al. Growth and Spectroscopy of Yb:$YMgB_5O_{10}$ Crystal. *Crystals* **2022**, *12*, 986. https://doi.org/10.3390/cryst12070986

Academic Editor: Jörg Fink

Received: 27 June 2022
Accepted: 12 July 2022
Published: 15 July 2022

Publisher's Note: MDPI stays neutral with regard to jurisdictional claims in published maps and institutional affiliations.

Copyright: © 2022 by the authors. Licensee MDPI, Basel, Switzerland. This article is an open access article distributed under the terms and conditions of the Creative Commons Attribution (CC BY) license (https://creativecommons.org/licenses/by/4.0/).

1. Introduction

The commercial availability of laser diodes based on InGaAs compounds in the Yb^{3+} absorption spectral range of 940 to 980 nm, together with the unique spectroscopic and laser properties of ytterbium-containing materials, has stimulated increased interest in the study of new crystalline solids with this activator for various types of lasers emitting near 1 μm. A simple two-level energy scheme of Yb^{3+} ions was shown to result in absence of losses due to excited state absorption, up-conversion and other concentration effects, as well as small differences in the energies of pump and generation photons, which ensured significantly lower heat release in the active laser medium, with a wide gain band making it possible to achieve effective high-power laser operation [1,2].

Many Yb^{3+}-doped crystals have previously been demonstrated. The spectroscopy and laser operation of Yb^{3+}-doped garnets [3–7], tungstates [8–13], vanadates [14–16], aluminates [17–25], phosphates [26–28], sesquioxides [29–31] and borates [32–38] have been reported. Tungstate crystals, such as Yb:KYW and Yb:KGW, are characterized by high absorption and stimulated emission cross-sections, as well as wide emission bands [9,39]; however, due to low thermal conductivity (~3 W/m·K) [40], the usage of these crystals in lasers with high average power is limited. The high thermal conductivity (up to 12 W/m·K [41,42]) of Yb-doped sesquioxides (Sc_2O_3, Lu_2O_3, Y_2O_3) makes them attractive

gain media for high-power lasers. However, the main disadvantage of these crystals is their high melting temperatures (>2400 °C) leading to difficulties in the production of bulk sesquioxide high-optical-quality material. Moreover, these crystals are characterized by narrow gain spectra and small absorption band widths (<3 nm). Borate crystals ($Ca_4YO(BO_3)_3$, $Ca_4GdO(BO_3)_3$, $Sr_3Y(BO_3)_3$) with trivalent ytterbium ions Yb^{3+} have wide gain bands and long fluorescence lifetimes of about 2.5 ms; however, these crystals have comparatively low absorption and stimulated emission cross-sections [8,27] and low thermal conductivity (~2 W/m·K) [43]. Yb:$YAl_3(BO_3)_4$ (YAB) oxoborate crystals have high thermal conductivity (~4.7 W/m·K), high absorption and emission cross-sections, as well as broad and smooth gain bands [44–48]. Borate crystals, such as $LaMgB_5O_{10}$, also have good thermal conductivity and optical properties [49,50]. $YMgB_5O_{10}$ (YMBO) borate crystals are considered as potential materials for the manufacture of laser matrices because they possess high thermal conductivity (6.2 ± 0.3 W/m·K) [51]. Yb^{3+}-doped YMBO single crystals have been grown using K_2O_3–MoO_3 and Li_2O– B_2O_3–LiF fluxes by a top-seeded solution growth method. Their structural, thermo-optical and spectroscopic properties were recently demonstrated [52].

In this manuscript, the growth details and characterization of a Yb:$YMgB_5O_{10}$ (YMBO) single crystal, as well as the results of its spectroscopic investigation, are reported. ATR-FTIR investigations in the far- and mid-IR ranges were performed for the first time.

2. Materials and Methods

A Yb:YMBO bulk crystal was grown using a high-temperature solution growth on dipped seeds (HT-SGDS) technique. Based on previously obtained results [53], a complex system, with composition 20 wt.% Yb:YMBO–80 wt.% $K_2Mo_3O_{10}$, was used in the growing experiment. Yb_2O_3 (99.96%), Y_2O_3 (99.96%), MgO (A.C.S. grade, produced by Aldrich, St. Louis, MO, USA), B_2O_3 (A.C.S. grade, produced by Alfa Aesar) were used as crystal-forming agents, which were weighed according to a composition of $Yb_{0.08}Y_{0.92}MgB_5O_{10}$. The solvent $K_2Mo_3O_{10}$ used was a mixture of K_2MoO_4 (A.C.S. grade, Chimkraft, Russia) and MoO_3 (A.C.S. grade, Aldrich production) which was weighed according to the following Equation:

$$K_2MoO_4 + 2MoO_3 = K_2Mo_3O_{10}.$$

Growth of the Yb:YMBO bulk crystal was performed in a vertical resistively heated furnace, equipped with a Proterm-100 precision temperature controller and a set of S-thermocouples. The temperature in the working zone of the furnace was maintained with a stability of ±0.1 °C.

The weighted materials were carefully mixed and ground, and then the growth charge was loaded into a Pt crucible, heated to 1000 °C, and held for 24 h to ensure a homogeneous solution. The choice of solvent composition for the single crystal growth experiments was based on previous results obtained for the spontaneous synthesis of YMBO crystals from a $K_2Mo_3O_{10}$ solvent. Spontaneous YMBO crystals, without obvious enclosure and cracking, which were previously obtained from a fluxed melt of similar composition, were selected and used as seeds for the growth experiments (Figure 1).

The saturation temperature of the high-temperature solution was estimated to be 880 °C by repeated observations of the growth/dissolution trial seed changes upon contact with the melt surface. The value obtained for the saturation temperature for the solute concentration being investigated was in good agreement with the solubility curve of $YMgB_5O_{10}$ in $K_2Mo_3O_{10}$ solvent described in [53], and was almost 100 °C lower than that reported [52]. During growth, supersaturation was maintained by cooling to 800 °C at a rate of 0.7 to 1.2 °C/day and followed by cooling to 300 °C at a rate of 10°/day. Finally, the grown crystal was removed from the furnace, cooled to room temperature for several days to prevent cracking due to heat shock, and then washed in hydrochloric acid.

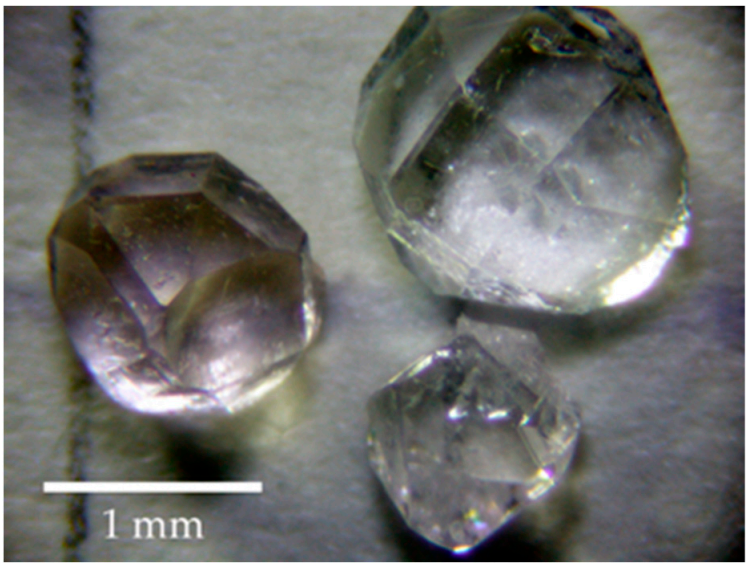


Figure 1. $YMgB_5O_{10}$ spontaneous crystals grown from $K_2Mo_3O_{10}$-based system.

Powder X-ray diffraction (PXRD) studies were carried out by means of a STOE STADI MP powder diffractometer (STOE &Cie GmbH, Darmstadt, Germany). A PXRD dataset was collected in continuous mode at room temperature using a CoK_α radiation source (λ = 1.7903 Å) in the range of 2θ = 3–90°. Phase identification was performed using the ICSD database and the Crystallography Open Database (COD) [54]. The unit cell parameters were calculated using 59 diffraction lines by means of DICVOL06 software implemented in the FullProf program package [55].

The chemical composition of the Yb:YMBO single crystal was carried using an analytical scanning electron microscope (SEM) technique using a JSM-IT-500 (JEOL Ltd., Akishima, Japan), equipped with the energy-dispersive X-ray (EDX) detector X-Max-n (Oxford Instruments Ltd., GB, Oxford, UK). The SEM was operated at an accelerating voltage of 20 kV and a probe current of 0.7 nA in high-vacuum mode. The sample was coated with a thin layer of carbon for the SEM investigations. B_K, Mg_K, Y_L and Yb_L lines in the EDS spectra were used for the elemental composition studies. The distribution coefficient of ytterbium (K_d) was defined as $K_d = C_c/C_d$, where C_c is the Yb content measured in the crystal and C_d is the concentration of Yb in the starting mixture.

Attenuated total reflection (ATR) spectra were measured with a BRUKER IFS 125HR Fourier spectrometer in the spectral range of 50–5000 cm^{-1} at room temperature. Measurements were carried out for two spectral ranges: in the far IR-range of 50–650 cm^{-1} using a Mylar beam-splitter, and in the mid-IR range of 400–5000 cm^{-1}, with a KBr beam-splitter. In both cases, a Globar was used as the radiation source. DTGS and DLATGS pyroelectric receivers were applied to record interferograms in the far- and mid-IR ranges, respectively.

Differential scanning calorimetry (DSC) and thermogravimetry analysis (TGA) were carried out by means of STA 449 F5 Jupiter® equipment (Netzsch, Germany) in the temperature range of 50–1500 °C with a heating rate of 20 K/min. PtRh20 85 μL crucibles were used in the DSC-TGA experiments. To clarify the thermal behavior of the investigated compound, Yb:YMBO crystals were thermally treated at 1150 °C for 1 h in a muffle furnace PVK-1.6-5 (Russia) equipped with a lanthanum-chromite-based heater. Products obtained after thermal processing were investigated using a PXRD method.

For spectroscopic investigations in polarized light, plates oriented along the three main optical axes of the N_g, N_m, and N_p were cut from the Yb:YMBO crystal. The polarized absorption spectra measurements were performed using a CARY 5000 spectrophotometer. The spectral bandwidth was ~0.4 nm.

The absorption cross sections $\sigma_{abs}(\lambda)$ were calculated according to (1):

$$\sigma_{abs}(\lambda) = \frac{k_{abs}(\lambda)}{N_{Yb}}, \quad (1)$$

where $k_{abs}(\lambda)$ is the absorption coefficient and N_{Yb} is the ytterbium concentration.

For investigation of luminescence kinetics, a β-$Ba_2B_2O_4$-based optical parametric oscillator was used. For registration of fluorescence, a monochromator MDR-12 (LOMO, St. Petersburg, Russia), an InGaAs photodiode with preamplifier and a 500 MHz digital oscilloscope were utilized. The luminescence registered in the spectral range of 950–1100 nm. As the exciting source, a laser diode emitting at near 960 nm was used. The spectra of luminescence radiation were measured using an MDR-23 monochromator (LOMO, St. Petersburg, Russia) and a PbS photoresistor supplied with a preamplifier connected to a Stanford Research Lock-In Amplifier SP830 (Stanford Research Systems, Sunnyvale, CA, USA).

3. Results and Discussion

3.1. Synthesis, Structure, and Composition

As a result of the HT-SGDS experiments undertaken, a transparent, colorless Yb-doped $YMgB_5O_{10}$ crystal with typical dimensions of about 25 × 23 × 25 mm and m = 10.337 g was grown (Figure 2).

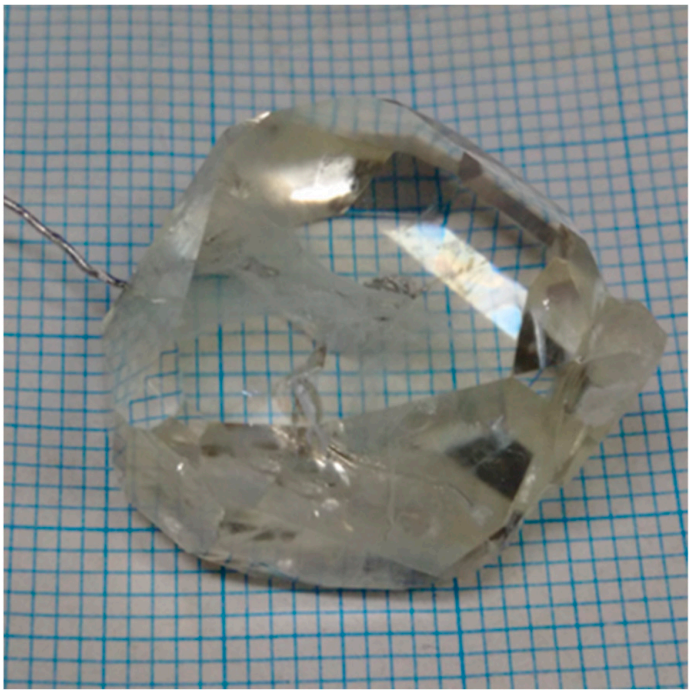


Figure 2. The Yb:$YMgB_5O_{10}$ single crystal grown in a 20 wt.% Yb: YMBO–80 wt.% $K_2Mo_3O_{10}$ system (1 mm scale).

The PXRD pattern of the Yb:YMBO crystal fitted well with that obtained for $YMgB_5O_{10}$ from the ICSD database (ICSD #4489) (Figure 3). The unit cell parameters, determined by indexing the X-ray powder pattern, were as follows: a = 8.532(2) Å, b = 7.580(2) Å, c = 9.360(2) Å, β = 93.70(2), V = 604.12 Å^3. The values obtained differed slightly from those of the authors of [52] because of the ytterbium alloy, but, in general, correlated well with them. The element content of the Yb:YMBO single crystal was measured at 11 points. The content of each chemical element corresponded to its stoichiometric ratio in the borate formula. From SEM-EDX analysis, the Yb concentration in the yttrium position was found to be 4.7 at.% with a distribution coefficient of K_d = 0.59. Therefore, the ytterbium

concentration N_{Yb} in the Yb:YMBO single crystal was calculated to be 3.71 × 10^{20} cm^{-3} using the measured volumetric density of 3.69 g/cm^3 [52].

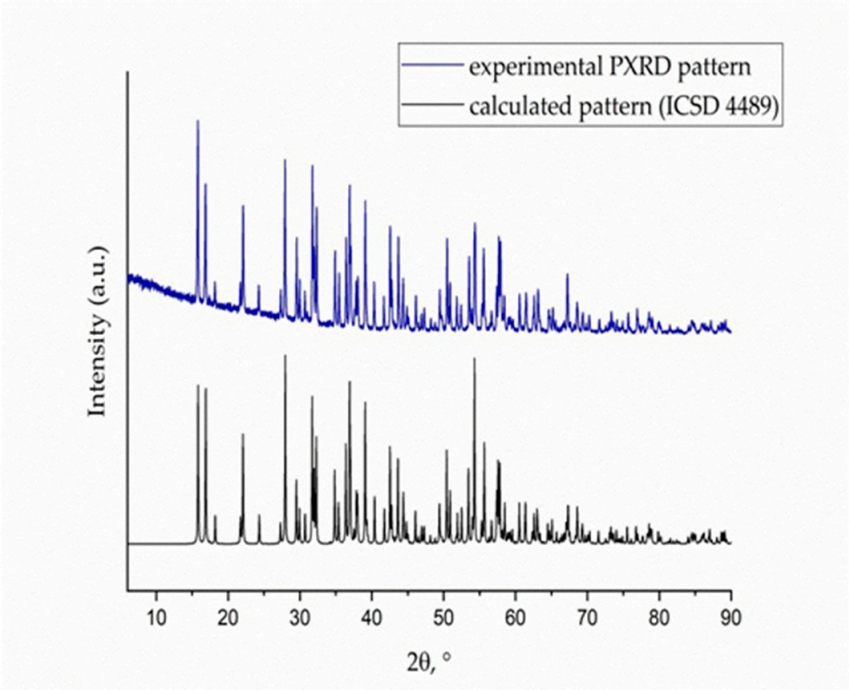


Figure 3. PXRD patterns for Yb:$YMgB_5O_{10}$ (blue) and calculated from *cif*-file for $YMgB_5O_{10}$, ICSD 4489 (black).

According to the structural data provided in [56], the unit cell (sp. gr. $P2_1/c$) of the $YMgB_5O_{10}$ compound contains $N = 68$ atoms ($Z = 4$), which corresponds to $3N = 204$ degrees of freedom. Three of these are associated with vibrations of the cell as a whole and are attributed to acoustic vibrations. Based on these structural data, a factor group analysis was carried out. All atoms of the investigated compound Y, Mg, B1–B5, O1–O10 were located in the position C_1. According to the symmetry of the positions of the atoms mentioned above and [57] each atom generated the following vibrations: $3A_g + 3A_u + 3B_g + 3B_u$. The resulting formula for the irreducible representations in the center of the Brillouin zone (Γ_{tot}) consists of acoustic (Γ_{acoust}), optical (Γ_{opt}), Raman active (*Raman*), and infrared active (*IR*) modes and has the following form:

$$\Gamma_{tot} = 51A_g + 51A_u + 51B_g + 51B_u \quad (2)$$

$$\Gamma_{acoust} = A_u + 2B_u \quad (3)$$

$$\Gamma_{opt} = 51A_g + 50A_u + 51B_g + 49B_u \quad (4)$$

$$Raman = 51A_g + 51B_g \quad (5)$$

$$IR = 50A_u + 49B_u \quad (6)$$

The ATR-FTIR spectrum of the Yb:YMBO crystal exhibited 37 strong phonons out of the 99 expected by factor group analysis (Figure 4). On the one hand, the missing phonons could not be resolved due to the large number of lattice vibrations with close frequencies in this complex compound. This scenario was confirmed by the appearance of a flat top in the peaks correlated with phonons near 325, 593, 877 cm^{-1}. On the other hand, absorption below 250 cm^{-1} due to intense phonons was observed. An analysis of the IR active phonon modes was previously reported in [56]. According to this study, vibrational modes between 1300–1500 cm^{-1} correspond to ν_{as} vibrations of $[BO_3]^{3-}$, ν_{as} vibrations of $[BO_4]^{5-}$ are in the range 1000–1200 cm^{-1}, and ν_s vibrations of $[BO_3]^{3-}$ are observed in the

region 800–1000 cm^{-1}. However, the authors of the study did not perform a factor group analysis and IR active phonons below 400 cm^{-1} were not determined.

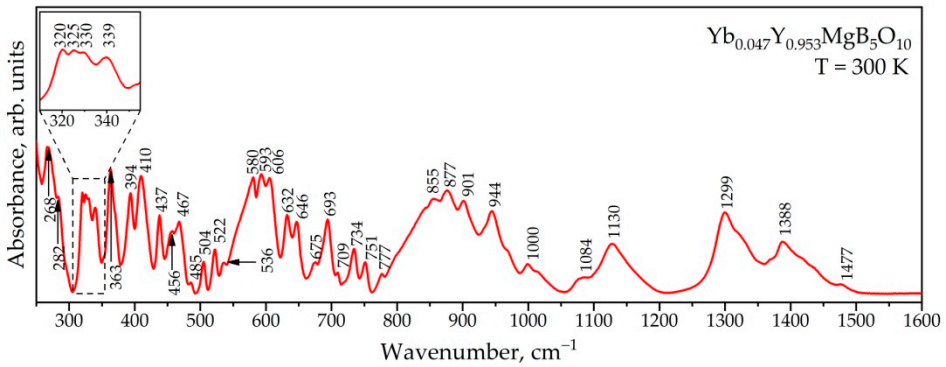


Figure 4. ATR-FTIR spectrum of Yb:YMBO in the range 250–1600 cm^{-1} at room temperature.

Data collected during TGA-DSC measurements in the temperature range 50–1500 °C are shown in Figure 5a,b. The DSC curve exhibits an endothermal peak at ~1051 °C. The absence of an exothermal peak on the cooling curve (insert on Figure 5a) and sample appearance suggest different thermal behavior from that described in [52]. The residue in the crucible after TGA-DSC measurements under heating up to 1100 °C was a white, opaque, dense mass. Repeated heating of the sample in the temperature range 50–1100 °C resulted in a small endothermic peak at ~1047 °C (Figure 5b), which may also indicate the decomposition of the studied compound. PXRD analysis revealed the existence of YBO_3 and $Mg_2B_2O_{10}$ (Figure 6).

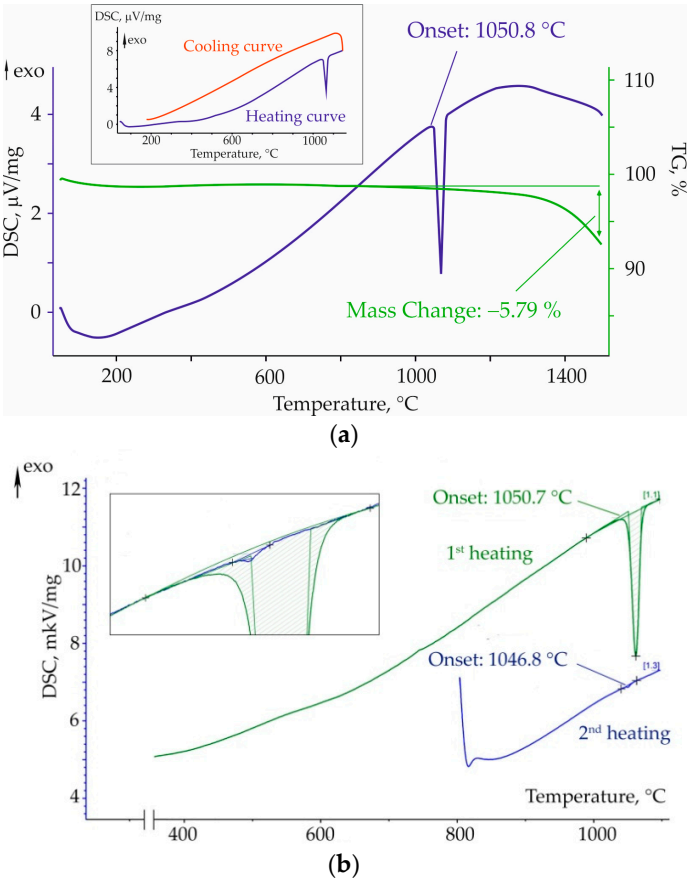


Figure 5. TGA-DSC curves of Yb:YMBO compound: (**a**) data collected in the temperature range of 50–1500 °C and (**b**) repeated heating in the temperature range 50–1100 °C.

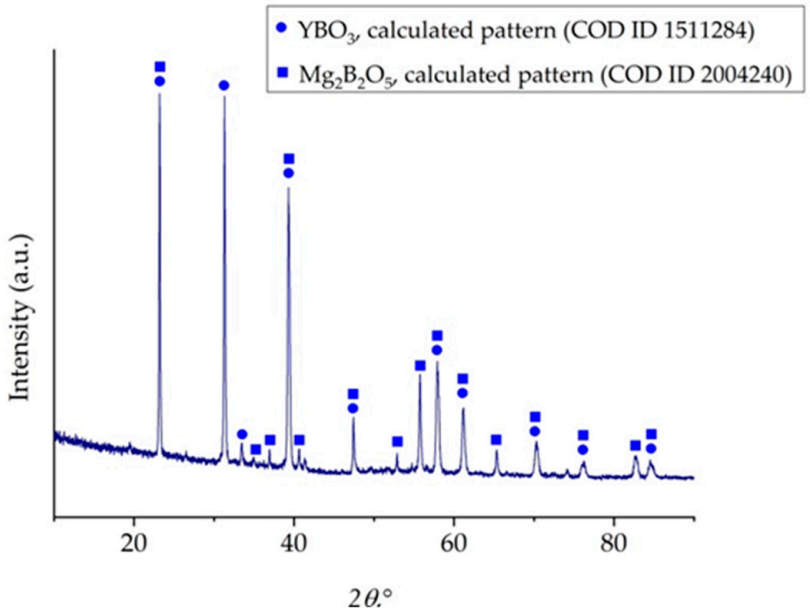


Figure 6. Powder X-ray diffraction pattern of products obtained after TGA-DSC experiments in the temperature range 50–1100 °C. PXRD analysis indicated the presence of YBO_3 and $Mg_2B_2O_{10}$ phases.

3.2. Spectroscopy

The obtained absorption cross-section spectra of the Yb:YMBO crystal are shown in Figure 7.

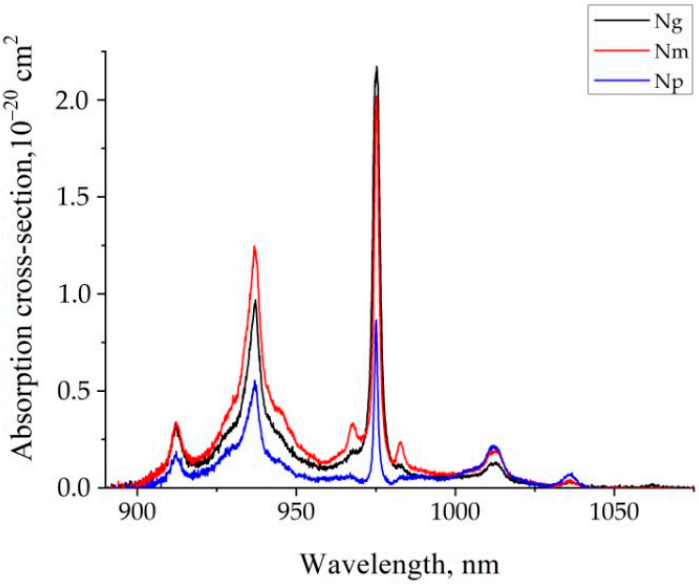


Figure 7. The absorption cross-section spectra of Yb^{3+}:YMBO crystal.

There were two intensive absorption lines centered at 937 nm and 975 nm. These wavelengths correspond to the emission spectra of commercially available InGaAs laser diodes. The maximal absorption cross-section was 2.15 × 10^{-20} cm^2 at 975 nm for the E//N_g axis. The comparatively narrow bandwidth (FWHM) of about 3 nm leads to additional requirements for thermal stabilization of the laser diode pumping. It is to be noted that there was a qualitative difference in the peaks' intensities in comparison with previously reported absorption spectra [52].

To reduce radiation trapping that can strongly influence the measured luminescence lifetime of Yb-doped materials, different methods can be applied [58,59]. In our case, a fine powder of Yb:YMBO crystal immersed in glycerin was used. The dependence of

the obtained lifetimes of the $^2F_{5/2}$ energy level on different weight content of Yb:YMBO crystalline powders in glycerin suspension is presented in Figure 8.

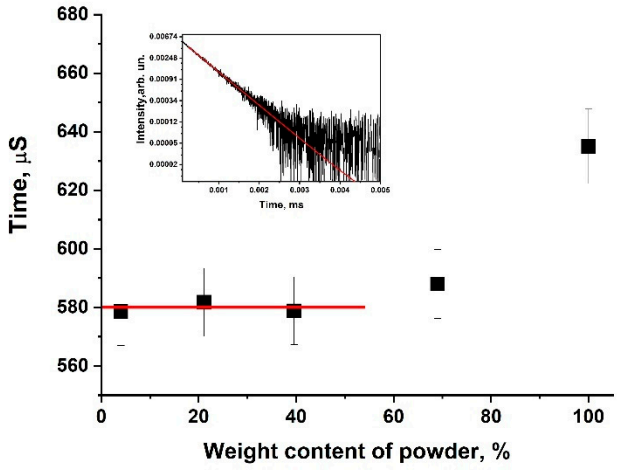


Figure 8. The $^2F_{5/2}$ energy level lifetimes of Yb: YMBO crystal. The inset shows the kinetics of luminescence decay from $^2F_{5/2}$ energy level of Yb^{3+} ions.

The inset in Figure 7 shows that the kinetics of luminescence decay from the $^2F_{5/2}$ energy level of Yb^{3+} ions were single exponential. A decrease in the $^2F_{5/2}$ energy level lifetime with decrease in the powder concentration in suspension was observed. Starting from ~40% weight content of powder, the lifetime did not change with further decrease in weight content, indicating little influence of reabsorption. As a result, the lifetime of the $^2F_{5/2}$ energy level was observed to be about 580 ± 10 μs (Figure 8). The luminescence lifetime obtained was shorter than that presented in [52], which can be explained in terms of the technique used that enabled better elimination of radiation trapping.

Considering the radiative lifetime of the $^2F_{5/2}$ Yb^{3+} level calculated in [52], the luminescence quantum yield was estimated to be about 0.87. The difference in the obtained value from 1, that is the usual case for Yb^{3+}-doped materials, can be explained by the large phonon energy in the borate crystals which promoted an effective non-radiative depletion of the upper Yb^{3+} ion energy level [48].

There were structured bands in the spectral range 950–1100 nm in the luminescence spectra of the Yb:YMBO crystal (Figure 9); these were generally in good agreement with the results presented in [52]. Two peaks, with maximal intensity at 1010 nm and 1040 nm for $E//N_m$, were observed in the luminescence spectrum of the Yb:YMBO crystal.

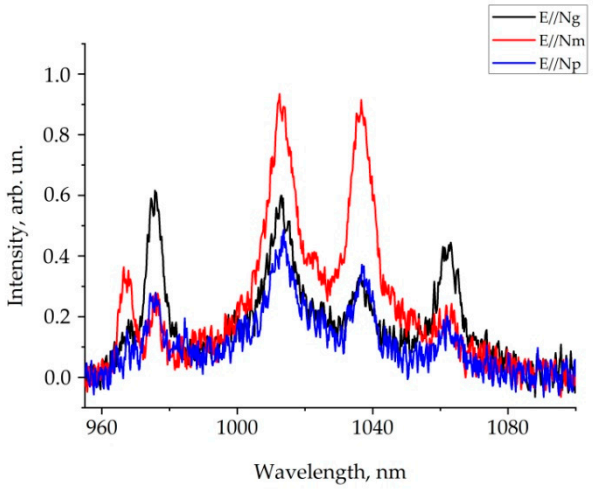


Figure 9. The luminescence spectrum of the Yb:YMBO crystal.

4. Conclusions

A transparent Yb:$YMgB_5O_{10}$ single crystal was grown using a high-temperature solution growth on dipped seeds technique with a $K_2Mo_3O_{10}$ solvent. The obtained crystal was characterized by means of PXRD, TGA-DSC and ATR-FTIR techniques. An investigation of the spectroscopic properties of the Yb:$YMgB_5O_{10}$ crystal was performed. Use of the crystal obtained for mode-locking and regenerative amplification will be addressed in future research.

Author Contributions: Writing—original draft preparation, A.I.L., K.N.G. and E.A.V.; formal analysis and investigation, A.I.L., K.N.G., A.S.Y., V.E.K., N.V.K., V.V.M., E.A.V., E.V.K., N.N.K., D.A.K., V.O.Y., D.D.M. and A.I.J.; writing—review and editing, N.V.K. and E.A.V. All authors have read and agreed to the published version of the manuscript.

Funding: This research received no external funding.

Institutional Review Board Statement: Not applicable.

Informed Consent Statement: Not applicable.

Data Availability Statement: Not applicable.

Conflicts of Interest: The authors declare no conflict of interest.

References

1. Krupke, W.F. Ytterbium solid-state lasers-the first decade. *IEEE J. Quant. Electron.* **2000**, *6*, 1287–1296. [CrossRef]
2. Brunner, F.; Spühler, G.J.; Aus der Au, J.; Krainer, L.; Morier-Genoud, F.; Paschotta, R.; Lichtenstein, N.; Weiss, S.; Harder, C.; Lagatsky, A.A.; et al. Diode-pumped femtosecondYb:$KGd(WO_4)_2$ laser with 1. 1-W average power. *Opt. Lett.* **2000**, *25*, 1119–1121. [CrossRef] [PubMed]
3. Reinberg, A.R.; Riseberg, L.A.; Brown, R.M.; Wacker, R.W.; Holton, W.C. GaAs: Si LED pumped Yb-doped YAG laser. *Appl. Phys. Lett.* **1971**, *19*, 11–16. [CrossRef]
4. Hönninger, C.; Paschotta, R.; Graf, M.; Morier-Genoud, F.; Zhang, G.; Moser, M.; Biswal, S.; Nees, J.; Braun, A.; Mourou, G.A.; et al. Ultrafast ytterbium-doped bulk lasers and laser amplifiers. *Appl. Phys. B* **1999**, *69*, 3–17. [CrossRef]
5. Haumesser, P.-H.; Gaumé, R.; Viana, B.; Vivien, D. Determination of laser parameters of ytterbium-doped oxide crystalline materials. *J. Opt. Soc. Am. B* **2002**, *19*, 2365–2375. [CrossRef]
6. Patel, F.D.; Honea, E.C.; Speth, J.; Payne, S.A.; Hutcheson, R.; Equall, R. Laser demonstration of $Yb_3Al_5O_{12}$ (YbYAG) and materials properties of highly doped Yb: YAG. *IEEE J. Quant. Electron.* **2001**, *37*, 135–144. [CrossRef]
7. Uemura, S.; Torizuka, K. Sub-40-fs pulses from a diode-pumped kerr-lens modelockedYb-doped yttrium aluminum garnet laser. *Jpn. J. Appl. Phys.* **2011**, *50*, 10201–10203. [CrossRef]
8. Brenier, A.; Boulon, G. Overview of the best Yb^{3+}-doped laser crystals. *J. Alloys Compd.* **2001**, *323*, 210–213. [CrossRef]
9. Kuleshov, N.V.; Lagatsky, A.A.; Podlipensky, A.V.; Mikhailov, V.P.; Huber, G. Pulsed laser operation of Yb-doped $KY(WO_4)_2$ and $KGd(WO_4)_2$. *Opt. Lett.* **1997**, *22*, 1317–1319. [CrossRef]
10. Demidovich, A.A.; Kuzmin, A.N.; Ryabtsev, G.I.; Danailov, M.B.; Strek, W.; Titov, A.N. Influence of Yb concentration on Yb:KYW laser properties. *J. Alloys Compd.* **2000**, *300*, 238–241. [CrossRef]
11. Mateos, X.; Petrov, V.; Aguilo, M.; Sole, R.M.; Gavalda, J.; Massons, J.; Diaz, F.; Griebner, U. Continuous-wave laser oscillation of Yb^{3+} in monoclinic $KLu(WO_4)_2$. *IEEE J. Quant. Electron.* **2004**, *40*, 1056–1059. [CrossRef]
12. Mateos, X.; Solé, R.; Gavaldà, J.; Aguiló, M.; Massons, J.; Díaz, F.; Petrov, V.; Griebner, U. Crystal growth, spectroscopic studies and laser operation of Yb^{3+}-doped potassium lutetium tungstate. *Opt. Mater.* **2006**, *28*, 519–523. [CrossRef]
13. Pujol, M.; Bursukova, M.A.; Güell, F.; Mateos, X.; Solé, R.; Gavaldà, J.; Aguiló, M.; Massons, J.; Díaz, F.; Klopp, P.; et al. Growth, optical characterization, and laser operation of a stoichiometric crystal $KYb(WO_4)_2$. *Phys. Rev. B* **2002**, *65*, 165121–165132. [CrossRef]
14. Haumesser, P.-H.; Gaumé, R.; Viana, B.; Antic-Fidancev, E.; Vivien, D. Spectroscopic and crystal-field analysis of new Yb-doped laser materials. *J. Phys. Condens. Matter* **2001**, *13*, 5427–5447. [CrossRef]
15. Kisel, V.E.; Troshin, A.E.; Tolstik, N.A.; Shcherbitsky, V.G.; Kuleshov, N.V.; Matrosov, V.N.; Matrosova, T.A.; Kupchenko, M.I. Spectroscopy and continuouswave diode-pumped laser action of Yb^{3+}:YVO_4. *Opt. Lett.* **2004**, *29*, 2491–2493. [CrossRef]
16. Sato, Y.; Saikawa, J.; Taira, T.; Nakamura, O.; Furukawa, Y. Spectroscopic properties of Yb:$GdVO_4$ single crystal: Stark levels, selection rules, and polarized cross sections. In *Advanced Solid-State Photonics*; Technical Digest Optical Society of America; Optica Publishing Group: Vienna, Austria, 2005; p. MF8. [CrossRef]
17. Weber, M.J. Optical properties of Yb^{3+} and Nd^{3+}-Yb^{3+} energy transfer in $YAlO_3$. *Phys. Rev. B* **1971**, *4*, 3153–3159. [CrossRef]
18. DeLoach, L.D.; Payne, S.A.; Chase, L.L.; Smith, L.K.; Kway, W.L.; Krupke, W.F. Evaluation of absorption and emission properties of Yb^{3+} doped crystals for laser applications. *IEEE J. Quant. Electron.* **1993**, *29*, 1179–1191. [CrossRef]

19. Zeng, X.; Zhao, G.; Xu, X.; Li, H.; Xu, J.; Zhao, Z.; He, X.; Pang, H.; Jie, M.; Yan, C. Comparison of spectroscopic parameters of 15at% Yb: $YAlO_3$ and 15at% Yb: $Y_3Al_5O_{12}$. *J. Cryst. Growth* **2005**, *274*, 106–112. [CrossRef]
20. Zhao, G.; Zeng, X.; Xu, J. Effects of Yb concentration on the fluorescence spectra of Yb-doped $YAlO_3$ single crystals. *Spectrochim. Acta Mol. Biomol. Spectrosc.* **2006**, *65*, 184–186. [CrossRef]
21. Wang, X.; Xu, X.; Zhao, Z.; Jiang, B.; Xu, J.; Zhao, G.; Deng, P.; Bourdet, G.; Chanteloup, J.-C. Comparison of fluorescence spectra of Yb:$Y_3Al_5O_{12}$ and Yb:$YAlO_3$ single crystals. *Opt. Mater.* **2007**, *29*, 1662–1666. [CrossRef]
22. Eichhorn, M. Quasi-three-level solid-state lasers in the near and mid infrared based on trivalent rare earth ions. *Appl. Phys. B* **2008**, *93*, 269–316. [CrossRef]
23. Boulon, G.; Guyot, Y.; Canibano, H.; Hraiech, S.; Yoshikawa, A. Characterization and comparison of Yb^{3+}-doped $YAlO_3$perovskite crystals (Yb:YAP) with Yb^{3+}-doped $Y_3Al_5O_{12}$ garnet crystals (Yb:YAG) for laser application. *J. Opt. Soc. Am. B* **2008**, *25*, 884–896. [CrossRef]
24. Petit, P.O.; Goldner, P.; Viana, B.; Boudeile, J.; Didierjean, J.; Balembois, F.; Druon, F.; Georges, P. Diode pumping of Yb^{3+}:$CaGdAlO_4$. In Proceedings of the International Conference on Lasers, Applications, and Technologies: Solid State Lasers and Amplifiers III, Strasburg, France, 16 April 2008; Volume 6998, pp. 1–6.
25. Li, D.; Xu, X.; Cheng, Y.; Cheng, S.; Zhou, D.; Wu, F.; Xia, C.; Xu, J.; Zhang, J. Crystal growth and spectroscopic properties of Yb:$CaYAlO_4$ single crystal. *J. Cryst. Growth* **2010**, *312*, 2117–2121. [CrossRef]
26. Brenier, A. A new evaluation of Yb^{3+}-doped crystals for laser applications. *J. Lumin.* **2001**, *92*, 199–204. [CrossRef]
27. Bayramian, A.J.; Bibeau, C.; Beach, R.J.; Marshall, C.D.; Payne, S.A.; Krupke, W.F. Three-level Q-switched laser operation of ytterbium-doped $Sr_5(PO_4)_3F$ at 985 nm. *Opt. Lett.* **2000**, *25*, 622–624. [CrossRef] [PubMed]
28. Schaffers, K.I.; Tassano, J.B.; Bayramian, A.B.; Morris, R.C. Growth of Yb: S-FAP [Yb^{3+}: $Sr_5(PO_4)_3F$] crystals for the Mercury laser. *J. Cryst. Growth* **2003**, *253*, 297–306. [CrossRef]
29. Petermann, K.; Huber, G.; Fornasiero, L.; Kuch, S.; Mix, E.; Peters, V.; Basun, S.A. Rareearth-doped sesquioxides. *J. Lumin.* **2000**, *89*, 973–975. [CrossRef]
30. Peters, V. Growth and Spectroscopy of Ytterbium-Doped Sesquioxides. Ph. D. Thesis, University of Hamburg, Hamburg, Germany, 2001.
31. Brenier, A.; Boulon, G. New criteria to choose the best Yb^{3+}-doped laser crystals. *Europhys. Lett.* **2001**, *55*, 647–652. [CrossRef]
32. Chénais, S.; Druon, F.; Balembois, F.; Georges, P.; Gaumé, R.; Haumesser, P.H.; Viana, B.; Aka, G.P.; Vivien, D. Spectroscopy and efficient laser action from diode pumping of a new broadly tunable crystal: Yb^{3+}:$Sr_3Y(BO_3)_3$. *J. Opt. Soc. Am. B* **2002**, *19*, 1083–1091. [CrossRef]
33. Földvári, I.; Beregi, E.; Baraldi, A.; Capelletti, R.; Ryba-Romanowski, W.; Dominiak Dzik, G.; Munoz, A.; Sosa, R. Growth and spectroscopic properties of rare-earth doped $YAl_3(BO_3)_4$ single crystals. *J. Lumin.* **2003**, *102*, 395–401. [CrossRef]
34. Wang, P.; Dawes, J.M.; Dekker, P.; Piper, J.A. Spectral properties and infrared laser performance of diode-pumped Yb:$YAl_3(BO_3)_4$. *Opt. Soc. Am.* **1999**, *26*, 614–617.
35. Liu, J.; Mateos, X.; Zhang, H.; Li, J.; Wang, J.; Petrov, V. High-power laser performance of Yb:$YAl_3(BO_3)_4$ crystals cut along the crystallographic axes. *IEEE J. Quant. Electron.* **2007**, *43*, 385–390. [CrossRef]
36. Aron, A.; Aka, G.; Viana, B.; Kahn-Harari, A.; Vivien, D.; Druon, F.; Balembois, F.; Georges, P.; Brun, A.; Lenain, N.; et al. Spectroscopic properties and laser performances of Yb:YCOB and potential of the Yb:LaCOB material. *Opt. Mater.* **2001**, *16*, 181–188. [CrossRef]
37. Wang, P.; Dawes, J.M.; Dekker, P.; Zhang, H.; Meng, X. Spectral characterization and diode-pumped laser performance of Yb:YCOB. *Opt. Soc. Am.* **1999**, *26*, 631–634. [CrossRef]
38. Druon, F.; Chénais, S.; Balembois, F.; Georges, P.; Brun, A.; Courjaud, A.; Hönninger, C.; Salin, F.; Zavelani-Rossi, M.; Augé, F.; et al. High-power diode-pumped Yb:GdCOB laser: From continuous-wave to femtosecond regime. *Opt. Mater.* **2002**, *19*, 73–80. [CrossRef]
39. Kuleshov, N.V.; Lagatsky, A.A.; Shcherbitsky, V.G.; Mikhailov, V.P.; Heumann, E.; Jensen, T.; Diening, A.; Huber, G. CW laser performance of Yb and Er, Yb doped tungstates. *J. Appl. Phys. B* **1997**, *64*, 409–413. [CrossRef]
40. Aggarwal, R.L.; Ripin, D.J.; Ochoa, J.R.; Fan, T.Y. Measurement of thermo-optic properties of $Y_3Al_5O_{12}$, $Lu_3Al_5O_{12}$, $YAIO_3$, $LiYF_4$, $LiLuF_4$, BaY_2F_8, $KGd(WO_4)_2$, and $KY(WO_4)_2$ laser crystalsin the 80–300 K temperature range. *J. Appl. Phys. B* **2005**, *98*, 103514. [CrossRef]
41. Peters, R.; Kränkel, C.; Fredrich-Thornton, S.T.; Beil, K.; Petermann, K.; Huber, G.; Heckl, O.H.; Baer, C.R.E.; Saraceno, C.J.; Südmeyer, T.; et al. Thermal analysis and efficient high power continuous-wave and mode-locked thin disk laser operation of Yb-doped sesquioxides. *J. Appl. Phys. B* **2011**, *102*, 509–514. [CrossRef]
42. Mun, J.H.; Jouini, A.; Yoshikawa, A.; Kim, J.-H.; Fukuda, T.; Lee, J. Thermal and optical properties of Yb-doped Lu_2O_3 single crystal grown by the micro-pulling-down method. *J. Ceram. Process* **2013**, *14*, 636–640.
43. Mougel, F.; Kahn-Harari, A.; Aka, G.; Pelenc, D. Structural and thermal stability of Czochralski grown GdCOBoxoborate single crystals. *J. Mater. Chem.* **1998**, *8*, 1619–1623. [CrossRef]
44. Blows, J.L.; Dekker, P.; Wang, P.; Dawes, J.M.; Omatsu, T. Thermal lensing measurements and thermal conductivity of Yb:YAB. *Appl. Phys. B* **2003**, *76*, 289–292. [CrossRef]
45. Wang, P.; Dawes, J.M.; Dekker, P.; Knowles, D.S.; Piper, A.J.; Lu, B. Growth and evaluation of ytterbium-doped yttrium aluminum borate as a potential self-doubling laser crystal. *J. Opt. Soc. Am. B* **1999**, *16*, 63–69. [CrossRef]

46. Liao, J.; Lin, Y.; Chen, Y.; Luo, Z.; Huang, Y. Flux growth and spectral properties of Yb:YAB single crystal with high Yb^{3+} concentration. *J. Cryst. Growth* **2004**, *267*, 134–139. [CrossRef]
47. Wang, P.; Dawes, J.M.; Dekker, P.; Piper, J.A. Highly efficient diode-pumped ytterbium-doped yttrium aluminum borate laser. *Opt. Commun.* **2000**, *174*, 467–470. [CrossRef]
48. Rudenkov, A.S.; Kisel, V.E.; Gorbachenya, K.N.; Yasukevich, A.S.; Maltsev, V.V.; Leonyuk, N.I.; Rubtsova, N.N.; Semyagin, B.R.; Kovalyov, A.A.; Preobrazhenskii, V.V.; et al. Growth, spectroscopy and high power laser operation of Yb:$YAl_3(BO_3)_4$ crystal: Continuous-wave, mode-locking and chirped pulse regenerative amplification. *Opt. Mater.* **2019**, *89*, 261–267. [CrossRef]
49. Huang, Y.S.; Zhou, W.W.; Sun, S.J.; Yuan, F.F.; Zhang, L.Z.; Zhao, W.; Wang, G.F.; Lin, Z.B. Growth, structure, spectral and laser properties of Yb^{3+}:$LaMgB_5O_{10}$—A new laser material. *CrystEngComm* **2015**, *17*, 7392. [CrossRef]
50. Huang, Y.S.; Chen, H.B.; Sun, S.J.; Yuan, F.F.; Zhang, L.Z.; Lin, Z.B.; Zhang, G.; Wang, G.F. Growth, thermal, spectral and laser properties of Nd^{3+}:$LaMgB_5O_{10}$ crystal—A new promising laser material. *J. Alloys Compd.* **2015**, *646*, 1083–1088. [CrossRef]
51. Mitina, D.D.; Maltsev, V.V.; Leonyuk, N.I.; Gorbachenya, K.N.; Deineka, R.V.; Kisel, V.E.; Yasukevich, A.S.; Kuleshov, N.V. Growth and characterization of $RMgB_5O_{10}$ (R=Y, La, Gd) crystals. *Inorg. Mater.* **2020**, *56*, 211–222. [CrossRef]
52. Sun, S.; Li, B.; Lou, F.; Shi, X.; Chen, W.; Yuan, F.; Zhang, L.; Lin, Z.; Zhong, D.; Huang, Y.; et al. Optimization of fluxes for Yb^{3+}:$YMgB_5O_{10}$ crystal growth and intense multi-wavelength emission characteristics in spectral and laser performances. *J. Mater. Chem.* **2021**, *9*, 14766. [CrossRef]
53. Maltsev, V.V.; Mitina, D.D.; Belokoneva, E.L.; Volkova, E.A.; Koporulina, E.V.; Jiliaeva, A.I. Synthesis and flux growth of rare-earth magnesium pentaborate crystals $RMgB_5O_{10}$ (R=Y, Gd, La, Tm and Yb). *J. Cryst. Growth* **2022**, *587*, 126628. [CrossRef]
54. *Inorganic Crystal Structure Data Base—ICSD*; Fachinformationzentrum (FIZ) Karlsruhe: Karlsruhe, Germany, 2021; Available online: https://www.crystallography.net/cod/ (accessed on 5 May 2022).
55. Boultif, A.; Louër, D. Powder pattern indexing with the dichotomy method. *J. Appl. Crystallogr.* **2004**, *37*, 724–731. [CrossRef]
56. Zhang, J.; Tao, X.; Cai, G.; Jin, Z. Phase relation, structure, and properties of borate $MgYB_5O_{10}$ in MgO–Y_2O_3–B_2O_3 system. *Powder Diffr.* **2017**, *32*, 97–106. [CrossRef]
57. Rousseau, D.L.; Bauman, R.P.; Porto, S.P.S. Normal mode determination in crystals. *J. Raman Spectrosc.* **1981**, *10*, 253–290. [CrossRef]
58. Sumida, D.S.; Fan, T.Y. Effect of radiation trapping on fluorescence lifetime and emission cross section measurements in solid-state laser media. *Opt. Lett.* **1994**, *19*, 1343–1345. [CrossRef] [PubMed]
59. Kühn, H.; Fredrich-Thornton, S.T.; Kränkel, C.; Peters, R.; Petermann, K. Model for the calculation of radiation trapping and description of the pinhole method. *Opt. Lett.* **2007**, *32*, 1908–1910. [CrossRef]